# Deep-lying hole states in nuclei: Microscopic approach

S. P. Klevansky and R. H. Lemmer
*Department of Physics and Nuclear Physics Research Unit, University of the Witwatersrand, Johannesburg, 2001, South Africa*
(Received 12 November 1982)

The strength function for deep-lying hole states in a nucleus is examined from a many-body point of view. Due to their interaction with the compound state background, such single hole excitations are interpreted as quasihole states that are not eigenstates of the nuclear Hamiltonian. These states show up as giant resonances in the strength function, with position and width determined by the real and imaginary parts of the quasihole energy. A formal theory of the strength and fragmentation of such states is developed by splitting the self-energy into background and doorway state contributions. The theory is applied to the calculation of the strength function for the isotopes of Sn using doorway states of a collective nature that consist of a hole plus collective vibrations of the target nucleus. A microscopic description of both the collective excitations and the hole state that it dresses is given in terms of a modified random phase approximation procedure that uses Green's functions for the individual single particle and single hole states that have been dressed by their interaction with the nuclear background. Specific calculations for the isotopes of Sn show good agreement with experiment.

[NUCLEAR STRUCTURE Theory of single hole strength function. Green's function method for optical potential; intermediate structure doorway states. Pairing, isospin. Calculations for isotopes of Sn.]

## I. INTRODUCTION

The problem we wish to study concerns itself with the properties of nuclear excited states that are reached by removing a nucleon from deep inside the Fermi sea. To the extent that the nucleus can be treated as an assembly of independent nucleons moving in a common shell model potential, such hole states continue to be very simple excitations that are created by removing a nucleon from one of the previously occupied shell model levels. This picture is of course an extreme oversimplification; if the hole state has a large binding energy, then its creation leads to an excited state of the residual nucleus lying anywhere from 5 to 15 MeV above its ground state. This places the single hole excitation in the vicinity of the much more complicated compound nucleus excitations of the nucleus, which have an increasingly high density of levels as the excitation energy increases. The interactions present in the full nuclear Hamiltonian couple the hole excitation to the many compound states that surround it, and cause its "strength" (i.e., single hole character) to be redistributed over the many compound states in its vicinity. A theoretical and experimental measure of this redistribution of the single hole character is provided by the strength function, which measures the probability per unit energy of finding the single hole state coupled to the compound states at a given excitation energy.

In this paper, we study the calculation of the strength function for deep-lying hole states. To this end, we exploit the important link between the single hole Green's function and the strength function, which is related to the imaginary part of the former. The construction of the Green's function, however, requires an exact solution of the full many-body problem. This is clearly a hopeless task. Therefore, we have to carry out some approximate construction of the Green's function in a fashion which emphasizes the main physical features of the problem. The ideas we describe next are suggested by the well-known successes of the optical model for particle scattering by atomic nuclei. In this situation one knows that the effect of the many degrees of freedom of the resulting compound nucleus can be approximately accounted for by introducing an absorptive component into the average field seen by the impinging nucleon.[1,2] Furthermore, one knows from empirical evidence from the so-called optical potentials that the imaginary part of the potential is of order 3% of the real part for low energy incoming nucleons. This corresponds to an excitation energy of 8 MeV in the compound nucleus, and shows that at even these excitation energies, the bulk of the (energy averaged) scattering is determined by the real part of the average nuclear potential. Since our discussion is directed toward the study of hole states, we have to adapt these ideas to single particle motion at negative energies. The concept of an average nuclear field for a hole continues to hold of course, and we accept that this field determines the main features of the hole state (binding energy, spin, and parity) in the spirit of the standard shell model. From Green's function theory, one knows that the effects of the nuclear medium on such a hole created in it are incorporated in terms of the single hole self-energy $\Sigma(\omega)$. The more formal aspects of the self-energy are discussed in Sec. II. However, it is useful at this stage to outline the physical ideas which form the basis of our approach. Consider a single hole state in the shell model. Its self-energy $\Sigma(\omega)$, excluding that already accounted for by the average shell model po-

 

tential, arises from the polarization effects the hole causes in the nuclear medium. Microscopically, these effects come about because the hole excites compound states lying near its own excitation energy. We split the contributions of such states into two parts, viz.,

$$\Sigma(\omega)=\Sigma^b(\omega)+\Sigma^d(\omega) .$$

The piece $\Sigma^b(\omega)$ describes the contribution to $\Sigma(\omega)$ arising from compound states that are strongly coupled to the hole state. We give arguments later to suggest that this contribution is slowly varying in energy and purely imaginary. The second piece $\Sigma^d(\omega)$ is the contribution from doorway states.[3] This represents a contribution to $\Sigma(\omega)$ coming from the coupling of the hole state to the compound states *locally* via a doorway in its vicinity. This piece is expected to have both real (dispersive) and imaginary (absorptive) contributions, and to vary rapidly with energy in the vicinity of the doorway states that it includes. Since we are dealing with reasonably high excitation energies, the contribution of $\Sigma^b(\omega)$ to the spreading of the single hole state is much larger than that from $\Sigma^d(\omega)$. The resulting quasihole state observed in the strength function therefore consists of a single giant resonance, whose width is determined by $\mathrm{Im}\Sigma^b(\omega)$, possibly fragmented into one or more intermediate structures due to poles in $\Sigma^d(\omega)$. Whether or not intermediate structure states become visible in the vicinity of such a quasihole giant resonance is determined by both the widths of the doorway states it couples to, and the strength of this coupling. This latter feature suggests that only doorway states having a collective nature present the possibility of showing up as intermediate structures.[4] Thus, in examining the spreading of a single hole state, we are led to consider doorway states having a one hole plus vibration structure, where the vibrational state is one of the collective states of the nucleus. We will see that the coupling matrix elements between the quasihole and such collective states have a coherent character, and are thus large.

From a microscopic point of view, such doorway states consist of a hole coupled to interacting particle-hole excitations which build up the collectivity.[5] Each of these particle-hole excitations are also spread out by their coupling to the nuclear compound states. Consequently, the Green's functions describing them have the same structure as the Green's function $G(\omega)$ we are trying to calculate. Thus one is faced with a self-consistency problem: the self-energy that enters $G(\omega)$ is in turn determined by the contributions $\Sigma^b(\omega)$ and $\Sigma^d(\omega)$ that in turn should enter the Green's functions determining these contributions. We break this impasse by the following argument. Since the contribution to the quasihole self-energy from $\Sigma^d(\omega)$ is much smaller than from $\Sigma^b(\omega)$ due to the localized (in energy) nature of the former, we simply neglect the contribution $\Sigma^d(\omega)$ to the dressing of the particles or holes making up the doorway state, and describe their propagation by a Green's function $G^b(\omega)$ that is only dressed with the self-energy $\Sigma^b(\omega)$.

Although the preceding assumptions result in an enormous simplification of the full many-body problem, their use in calculating $\Sigma^d(\omega)$ presents one with further problems, since the actual energy dependence of $G^b(\omega)$ enters the construction of the self-energy in an essential way. Therefore, to actually do such calculations, we have made appeal to the approximate procedures developed by Dover *et al.*,[6] which we have extended and developed further so as to be applicable to the much more general problem of quasihole damping.

The use of a dressed Green's function $G^b(\omega)$ introduces new features into the construction of the collective mode part of the doorway states, which we construct in the random phase approximation[5] (RPA). The resulting RPA eigenvalue problem now develops complex eigenvalues, which in addition are a function of the energy $\omega$, necessitating a study of this problem in conjunction with its adjoint.

We find that it is possible to implement the above procedures without making a specific choice as to how the background self-energy $\Sigma^b(\omega)$ behaves with energy, as long as this variation is a slow one. The results we obtain for the composite self-energy also retain the general features expected of it as a function of $\omega$. In particular, we find that our approximations preserve the very important property of $\mathrm{Im}\Sigma(\omega)$ changing sign as the energy variable $\omega$ passes through the Fermi level. The other important result that follows from using $G^b(\omega)$ in calculating the doorway state self-energy is that it automatically endows the doorway states with a width that is also determined from $\Sigma^b(\omega)$. Thus the widths of the giant resonance and the intermediate structure resonances are determined by one and the same function.

We have chosen the isotopes of Sn as a specific case to illustrate the results of this formalism, which is quite general. The reasons for this choice are twofold: on the theoretical side, the nuclear structure of these isotopes is well understood, and their hole strength functions have been extensively investigated experimentally, most recently by Gerlic *et al.*[7] The actual implementation of this formalism involves additional assumptions and technical complications due to the structure of these nuclei. The main additional assumption that must be introduced is a specific parametrization of $\Sigma^b(\omega)$, and a recognition that pairing and isospin effects play an essential role in the Sn isotopes. These matters are taken up in Secs. V and VI. Specific results are shown in Sec. VII for the $g_{9/2}$ quasihole in Sn. We comment in detail in Sec. VI on the underlying assumptions leading to these results. Suffice it to say that the fits we obtain in comparison with the experimental data are excellent, and therefore suggest that the spreading mechanism introduced into the shell model via the self-energy having background and doorway contributions, has isolated the main physical features of the problem.

## II. FORMALISM

### A. The Green's function

The resonance structure in the strength function associated with a hole state which is formed by the removal of a particle from an $A$-nucleon system, can be investigated us-

ing the single particle Green's function $G_{12}(\omega)$ in Fourier space. $G_{12}(\omega)$ is known to satisfy a Dyson equation,

$$G_{12}(\omega)=G_{12}^{(0)}(\omega)+\sum_{34} G_{13}^{(0)}(\omega)\Sigma_{34}(\omega)G_{42}(\omega)\ . \qquad (2.1)$$

Here $\Sigma_{34}(\omega)$ is the self-energy describing the effects of the nuclear medium on the particle or hole. The numerical state labels used are arbitrary insofar as one is free to choose the representation in which to calculate $G_{12}(\omega)$. The physical situation we wish to consider is how a single hole state created in the nucleus is affected by its interaction with the more complicated excitations to which it is coupled. One knows that, if possible excitations of the nucleus are put aside, the effect of the remaining nucleons on the motion of a nucleon in the nucleus is adequately described by an average field. This field can either be represented phenomenologically by a shell model potential, or approached theoretically as in Hartree-Fock theory. In this paper, we take the latter approach in principle, and interpret the labels in Eq. (2.1) as referring to Hartree-Fock (HF) states of a single nucleon. This means that all effects of exciting the nuclear medium through which a nucleon or nucleon hole is moving, reside in $\Sigma_{34}(\omega)$. With this choice of representation, $G_{12}^{(0)}(\omega)$ is dressed to the extent that interactions with the average nuclear field have been taken into account. Consequently, it is diagonal in the labels 1 and 2: $G_{12}^{(0)}(\omega)=G_1^{(0)}(\omega)\delta_{12}$. The same statement does not hold true for $G_{12}(\omega)$, however, since the particle in state 2 can scatter into state 1 by exciting the nuclear medium. In a spherically symmetric average field, labels 1 and 2 differ at most in their radial quantum numbers. However, radial excitations involve energies of order twice the average spacing between major shells ($\sim$20 MeV in a typical nucleus, $A=100$). Since the two nucleon scattering matrix elements are generally much smaller than this, the feature of a large energy gap between shells allows us to replace $\Sigma_{34}(\omega)$ by its diagonal elements only. The resulting Dyson equation for $G_{12}(\omega)=G_1(\omega)\delta_{12}$ may then be solved explicitly to obtain

$$G_1(\omega)=[G_1^{(0)^{-1}}(\omega)-\Sigma_1(\omega)]^{-1}\ . \qquad (2.2)$$

In particular, the Green's function $G_1^{(0)}(\omega)$ for a particle or hole in the HF state 1 of energy $\epsilon_1$ is given by[8]

$$G_1^{(0)}(\omega)=\left[\frac{1-n_1}{\omega-\epsilon_1+i\eta}+\frac{n_1}{\omega-\epsilon_1-i\eta}\right],\quad \eta\to 0^+\ , \qquad (2.3)$$

where the HF occupation number $n_1=0$ or 1, depending on whether $\epsilon_1$ lies above or below the Fermi surface at energy $\lambda$. Inserting this into Eq. (2.2) yields the familiar result

$$G_1(\omega)=[\omega-\epsilon_1-\Sigma_1(\omega)]^{-1}\ . \qquad (2.4)$$

Thus, in order to calculate $G_1(\omega)$, a knowledge of the self-energy $\Sigma_1(\omega)$ is required.

### B. The nucleon self-energy

We now examine the exact expression for the nucleon self-energy. Apart from a static (HF) contribution, which has already been taken into account, this is given by[9,10]

$$\Sigma(\omega)=\tfrac{1}{2}\int_{-\infty}^{\infty}\frac{d\omega'}{2\pi}\int_{-\infty}^{\infty}\frac{d\omega''}{2\pi}\tilde{V}G(\omega-\omega')G(\omega'+\omega'')G(\omega'')\Gamma(\omega,\omega',\omega'')\ , \qquad (2.5)$$

where the summations over intermediate states are implied. Here $\tilde{V}$ and $\Gamma$ are the fully antisymmetrized two-body interaction and four point vertex function, respectively. The factor $\frac{1}{2}$ in Eq. (2.5) compensates for the double counting introduced by antisymmetrizing both the initial and final interaction vertices. The $G$'s are exact Green's functions as given by Eq. (2.1). Their frequency arguments are determined by energy conservation requirements. A convenient choice of these is shown in Fig. 2.

The vertex function $\Gamma$ summarizes the effect of all possible interactions between two noninteracting but fully dressed nucleon lines propagating according to the exact Green's function of Eq. (2.1). It can be shown[10] that the structure of the integral equation for $\Gamma$ depends on which vertex labels are identified with incoming and outgoing states. In the event that (1,2) represent incoming and (3,4) outgoing states, one obtains the integral equation shown diagrammatically in Fig. 1.

The vertical double line indicates an (antisymmetrized) effective interaction that is irreducible with respect to the labels (1,2) and (3,4). The vertex function is in general a function of three energy variables, $\Gamma=\Gamma(\omega,\omega',\omega'')$. However, if the effective interaction in Fig. 1 is approximated by $\tilde{V}$, the resulting integral equation shows that this $\Gamma$ is only a function of the energy variable $\omega'$. Thus, writing $\Gamma(\omega')$ in place of $\Gamma(\omega,\omega',\omega'')$, one finds upon translating[11] the diagrams in Fig. 1 into symbols, the following relation:

$$\Gamma(\omega')=\tilde{V}-i\int\frac{d\tilde{\omega}}{2\pi}\Gamma(\omega')G(\tilde{\omega}+\omega')G(\tilde{\omega})\tilde{V} \qquad (2.6)$$

$$=\tilde{V}-\Gamma(\omega')\Pi(\omega')\tilde{V}\ . \qquad (2.7)$$

In this expression, we have retained the approximation, already motivated in Sec. II A, that the Green's functions are diagonal in their state labels. Equation (2.7) gives the

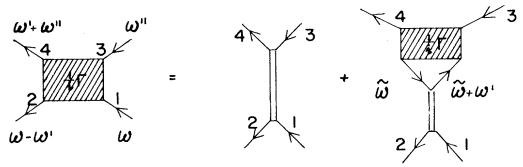


FIG. 1. Integral equation for the vertex function $\Gamma$. The effective interaction is indicated by vertical double lines.

effective interaction $\Gamma$ in the random phase approximation (RPA). This can be seen by iterating the equation on $\tilde{V}$. The result is a series of bubble diagrams (each bubble represented by $-i\Pi$) connected by the direct and exchange matrix elements.

We now return to the exact expression for $\Sigma$, and insert the $\Gamma$ obtained from Eq. (2.7). Since this vertex function is only a function of $\omega'$, the energy integral over $\omega''$ in Eq. (2.5) generates a noninteracting polarization propagator again. One finds

$$\Sigma(\omega)=-\frac{i}{2}\int\frac{d\omega'}{2\pi}G(\omega-\omega')\tilde{V}\Pi(\omega')\Gamma(\omega')\ . \tag{2.8}$$

The meaning of this approximation becomes clear if one inserts $\Gamma(\omega')$ in terms of the integral equation it satisfies. Then, carrying state labels explicitly,

$$\Sigma(\omega)=-\frac{i}{2}\sum_{23456}\int\frac{d\omega'}{2\pi}G_2(\omega-\omega')(51\mid\tilde{V}\mid 62)F(6543,\omega')(62\mid\tilde{V}\mid 51)\ , \tag{2.9}$$

where

$$F(6543,\omega')=\Pi(34,\omega')\delta_{36}\delta_{45}-\Pi(65,\omega')(64\mid\Gamma(\omega')\mid 53)\Pi(34,\omega') \tag{2.10}$$

is the polarization propagator for particle-hole pairs interacting via $\Gamma$. In the same way that $\Gamma(\omega')$ was shown to be the effective interaction in RPA, its presence in this expression gives the RPA version of $F$. In actual applications, where a simple form of effective interaction will be used, we will ignore the antisymmetry of $\tilde{V}$ and $\Gamma$, and therefore drop the factor $\frac{1}{2}$ in Eq. (2.9).

The approximation (2.9) has a simple graphical interpretation. This is shown in Fig. 2. The exact expression for $\Sigma(\omega)$ has been replaced by one in which the intermediate nucleon state is modified by attaching the RPA version of the interacting particle-hole propagator to it.

### C. Background and doorway stage contributions

We now identify two types of contributions to $\Sigma$ by making use of known features of nuclear structure. Since $G$ and $F$ in Eq. (2.9) are still essentially exact propagators, one knows that they vary rapidly with their energy arguments, the former having poles at the excitation energies of the $A\pm1$ particle systems, the latter at the excitation energies of the $A$ particle system. The energy-averaged versions of these two propagators over the actual energy spectrum are expected to be smooth functions of $\omega$, however. Then $G(\omega)$ describes the propagation of a dressed particle or hole state with an energy and width given by the (complex) poles of the averaged $G$, while the poles of the averaged $F(\omega)$ describe the eigenmode vibrations of such interacting dressed particle-hole pairs. These vibrations are of two types: collective and noncollective. Of these, one anticipates that only those vibrational modes in $F$ that are of a collective character will induce prominent energy dependent features in $\omega$, with the noncollective modes contributing to a smoothly varying background. Let us denote the latter contribution to $\Sigma$ by $\Sigma^b$. In contrast, the collective piece of $F$ is coupled to an intermediate dressed state in the manner depicted in Fig. 2, to provide doorway states of a dressed single particle state plus vibration character, thus making up a doorway contribution. We denote this contribution to $\Sigma$ by $\Sigma^d$. Hence,

$$\Sigma_1(\omega)=\Sigma_1^b(\omega)+\Sigma_1^d(\omega)\ . \tag{2.11}$$

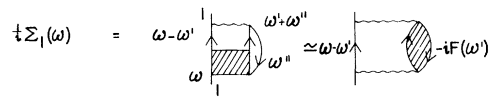


FIG. 2. Exact form of the self-energy and its approximation in terms of a nuclear polarization diagram.

### D. The background self-energy

The bulk of the effect of residual interactions on a nucleon state in the average potential is accounted for by including an imaginary part in this average potential. This circumstance is brought about by the fact that, in the strong coupling limit, the strength of the single particle state at energy $\epsilon_1$ is distributed fairly uniformly over the many compound states to which it is coupled. One can then anticipate that the real part of the piece $\Sigma^b$, when *averaged* over the compound states surrounding $\epsilon_1$, will vanish, leaving a purely imaginary contribution.[12] We can thus set

$$\Sigma_1^b(\omega=\mp iW_1(\omega)\ \text{ for } \omega\gtrless\lambda\ , \tag{2.12}$$

where we treat the matrix element

$$W_1(\omega)=\langle 1\mid W_{\rm opt}(\omega)\mid 1\rangle$$

as a phenomenological function. The sign change as $\omega$ passes through the Fermi surface is required by general theory.[8] Equation (2.12) therefore identifies $\Sigma_1^b(\omega)$ with the imaginary part $W_{\rm opt}(\omega)$ of the nuclear optical potential, but taken at values of its argument that do not necessarily lie on the energy shell, $\omega=\epsilon_1$. The phenomenology of this potential has been well documented for positive on-shell energy arguments.[2] In what follows, we will require $W_{\rm opt}(\omega)$, or rather its matrix elements, at *negative* energies, about which much less is known empirically. We take up this question in Sec. VI. Irrespective of such detail, Eq. (2.12) has the following implications: if 1 is a particle state $p$ with energy $\epsilon_1>\lambda$, then $W_p(\omega)$ is to be identified with $\langle p\mid W_{\rm opt}(\omega)\mid p\rangle$ for all $\omega>\lambda$. Since $\omega$ ranges over all values both greater and less than $\lambda$, this interpretation can only be maintained if $W_p(\omega)$ is set identi-

cally to zero for all $\omega<\lambda$. Similarly for hole states, $\epsilon_1<\lambda$,

$$W_h(\omega)=\langle h \mid W_{\rm opt}(\omega) \mid h\rangle$$

for $\omega<\lambda$ and zero otherwise. If we further insist that $W_1(\lambda)=0$ for $1=p$ or $h$, a condition borrowed from Fermi liquid theory,[13] then a consistent phenomenological description of $\Sigma_1^b(\omega)$ is obtained that is summarized by the equation

$$\Sigma_1^b(\omega)=-i(1-n_1)W_1(\omega)\theta(\omega-\lambda)+in_1W_1(\omega)\theta(\lambda-\omega)\ . \tag{2.13}$$

The $\theta$'s are step functions.

### E. Doorway states

The arguments leading up to Eq. (2.13) are valid as long as the strong coupling approximation holds. This is not the case if the coupling to compound states occurs via doorway states.[3] Then a different situation prevails. Instead, the strength of the state 1 is fragmented over the doorway states it is coupled to. Since the doorway states are themselves spread only locally into compound states in their vicinity, an indirect coupling between state 1 and the compound states is effected. The cancellation of the real part of the energy-averaged contribution to the self-energy no longer occurs, so that the piece $\Sigma_1^d(\omega)$ arising from doorway state excitations has both real and imaginary contributions to $\Sigma_1(\omega)$. In what follows, we use Eq. (2.9) to calculate the doorway self-energy $\Sigma^d$ using a specific nuclear model.

Although the expression (2.9) with $G$ and $F$ interpreted as energy averaged propagators is a highly simplified version of the exact result, there is yet a further complication in that these propagators required to calculate $\Sigma^d$ still depend on $\Sigma$ itself. We resolve this problem using the following argument. Since doorway states of a collective nature are expected to be relatively few in number, the bulk of the self-energy that converts a Hartree-Fock state into a dressed state is given by $\Sigma^b$. Consequently, we dress all nucleon lines by including only $\Sigma^b$ in the single particle propagator,

$$G_1(\omega)\cong G_1^b(\omega)=[\omega-\epsilon_1-\Sigma_1^b(\omega)]^{-1} \tag{2.14}$$

in evaluating expressions like (2.7) and (2.9).

Several alternative approaches to the problem of damping of single particle modes in nuclei have been discussed elsewhere.[14]

## III. POLARIZATION PROPAGATORS

In this section we construct explicit expressions for the (averaged) polarization propagators $\Pi$ and $F$ pertaining to noninteracting and interacting dressed particle-hole pairs, respectively.

### A. The noninteracting particle-hole propagator

The propagator $\Pi$ for noninteracting particle-hole pairs appears in Eq. (2.7). This expression corresponds graphically to a single bubble diagram containing fully dressed particle and hole lines. An evaluation of $\Pi$ can be carried out using the Lehmann representation[9] that expresses the $G$'s in terms of the excitation energies $\epsilon_s$ and $\epsilon_{s'}$, and strength functions of the $A\pm1$ particle systems. One has, in particular, the relation

$$\mathrm{Im}G_1(\omega)=-\frac{\pi}{D_s}\overline{|(c_1^\dagger)_{s0}|^2}_{\epsilon_s=\omega-\lambda}\theta(\omega-\lambda)+\frac{\pi}{D_{s'}}\overline{|(c_1)_{s'0}|^2}_{\epsilon_{s'}=\lambda-\omega}\theta(\lambda-\omega) \tag{3.1}$$

if the $\epsilon_s$ and $\epsilon_{s'}$ are quasicontinuously distributed with average spacings $D_s$ and $D_{s'}$. We have set

$$(c_1^\dagger)_{s0}=\langle\Phi_s^{A+1}\mid c_1^\dagger\mid\Phi_0^A\rangle\ ,$$

etc., using an obvious notation, and the bars denote energy averages in the vicinity of $\epsilon_s=\omega-\lambda$ and $\epsilon_{s'}=\lambda-\omega$, respectively. One finds by direct calculation that $\Pi(12,\omega)$ is given in terms of these quantities as

$$\Pi(12,\omega)=-\int_0^\infty\frac{1}{D_s}d\epsilon_s\int_0^\infty\frac{1}{D_{s'}}d\epsilon_{s'}\frac{\overline{|(c_1^\dagger)_{s0}|^2}\,\overline{|(c_2)_{s'0}|^2}}{\omega-\epsilon_s-\epsilon_{s'}+i\eta}+(1\to2,\omega\to-\omega)\ . \tag{3.2}$$

As a prelude to evaluating this expression, we identify the strength functions $\overline{|(c_1^\dagger)_{s0}|^2}$ and $\overline{|(c_2)_{s'0}|^2}$ as arising from the background contribution of compound levels. Therefore, by taking the imaginary part of $G_1^b(\omega)$, one finds that the strength functions are given by

$$\frac{\pi}{D_s}\overline{|(c_1^\dagger)_{s0}|^2}=\frac{W_1(\epsilon_s+\lambda)}{(\epsilon_s-\epsilon_1+\lambda)^2+W_1^2(\epsilon_s+\lambda)}(1-n_1)\ , \tag{3.3}$$

$$\frac{\pi}{D_{s'}}\overline{|(c_2)_{s'0}|^2}=\frac{W_2(\lambda-\epsilon_{s'})}{(\epsilon_{s'}+\epsilon_2-\lambda)^2+W_2^2(\lambda-\epsilon_{s'})}n_2 \tag{3.4}$$

as long as $\epsilon_1>\lambda$ and $\epsilon_2<\lambda$.

An explicit evaluation of $\Pi$ using these expressions is prevented by the unknown dependence of $W_1$ and $W_2$ on their energy arguments. However, the resonance forms in $\epsilon_s$ and $\epsilon_{s'}$ of the strength functions plus the fact that the integrand is singular at $\epsilon_s+\epsilon_{s'}=\omega$ suggests the following approximate procedure[6]: replacing $W_1(\epsilon_s+\lambda)$ and $W_2(\lambda-\epsilon_{s'})$ by their values where the integrand in Eq. (3.2) is large. These values occur where, simultaneously, $\epsilon_s+\epsilon_{s'}=\omega$ and the product $\overline{|(c_1^\dagger)_{s0}|^2}\,\overline{|(c_2)_{s'0}|^2}$ is large. This in turn happens when either of the expressions (3.3) or (3.4) resonates. Thus while maintaining the condition $\epsilon_s+\epsilon_{s'}=\omega$, we must evaluate $W_1(\lambda+\epsilon_s)$ in the particle strength function at the peak $\epsilon_{s'}=\lambda-\epsilon_2$ of the hole strength function, and $W_2(\lambda-\epsilon_{s'})$ in the hole strength function at the peak $\epsilon_s=\epsilon_1-\lambda$ of the particle strength

function. One then finds that the $W$'s in Eqs. (3.3) and (3.4) must be replaced by $W_1(\epsilon_2+\omega)$ and $W_2(\epsilon_1-\omega)$. The resulting integrals for $\Pi$ now become elementary, if we extend the lower limits to $-\infty$. This is justified by the peaked nature of the strength functions. Thus

$$\Pi(12,\omega)=\frac{(1-n_1)n_2}{\epsilon_1-\epsilon_2-i[W_1(\epsilon_2+\omega)+W_2(\epsilon_1-\omega)]-\omega}+(1\rightarrow 2,\omega\rightarrow-\omega)\ . \tag{3.5}$$

We remark in passing that the approximate strength functions obtained by replacing the energy-dependent $W$'s by constants with respect to $\epsilon_s$ and $\epsilon_{s'}$ still satisfy the sum rule

$$\sum_s |(c_1^\dagger)_{s0}|^2+\sum_{s'} |(c_1)_{s'0}|^2=1$$

in the sense that, individually, one finds

$$\sum_s |(c_1^\dagger)_{s0}|^2\cong\frac{1}{D_s}\int_{-\infty}^{\infty} d\epsilon_s\,\overline{|(c_1^\dagger)_{s0}|^2}=1-n_1\ ,$$
$$\sum_{s'} |(c_1)_{s'0}|^2\cong\frac{1}{D_{s'}}\int_{-\infty}^{\infty} d\epsilon_{s'}\,\overline{|(c_1)_{s'0}|^2}=n_1\ . \tag{3.6}$$

### B. The interacting particle-hole propagator

The expression for $F$ in Eq. (2.10) can be written as

$$F(4321,\omega)=\Pi(43,\omega)\left[\delta_{14}\delta_{23}-\sum_{56}(54\mid V\mid 63)F(6521,\omega)\right] \tag{3.7}$$

with the help of the integral equation for $\Gamma$. The structure of Eq. (3.7) is such as to couple those matrix elements of $F(4321,\omega)$ where the index pairs (4,3) and (2.1) are either particle-hole or hole-particle states. Thus $F$ breaks up into submatrices labeled by the type of excitation these indices represent. After substituting for $\Pi(43,\omega)$, Eq. (3.7) can be arranged as a matrix equation,

$$\begin{bmatrix} A-i\Gamma(\omega)-\omega I & B \\ B^* & A^*-i\Gamma(-\omega)-\omega I \end{bmatrix}\begin{bmatrix} F_{ph,hp} & F_{ph,ph} \\ F_{hp,hp} & F_{hp,ph}\end{bmatrix}=\begin{bmatrix} I & 0\\ 0 & I\end{bmatrix} \tag{3.8}$$

in this space. We employ the now standard notation[5] $A$ and $B$ for the matrices $A_{mi,nj}=E_{mi}\delta_{mn}\delta_{ij}+(jm\mid\tilde{V}\mid ni)$ and $B_{mi,nj}=(mn\mid\tilde{V}\mid ij)$. $A$ is Hermitian, $B$ is symmetric, and $I$ is the unit matrix. The excitation energies and half-widths of the participating particle-hole excitations are $E_{mi}=(\epsilon_m-\epsilon_i)$ and $\Gamma_{mi}(\omega)=W_m(\epsilon_i+\omega)+W_i(\epsilon_m-\omega)$. If $\Gamma_{mi}\rightarrow 0$, one recovers the standard RPA equations.[5]

We solve for the matrix $F$ by inverting Eq. (3.8) in terms of the eigenvalues and eigenvectors of the associated homogeneous problem. At *fixed* $\omega$ this reads

$$\begin{bmatrix} A-i\Gamma(\omega) & B \\ B^* & A^*-i\Gamma(-\omega)\end{bmatrix}\begin{bmatrix} X_\lambda(\omega)\\ Y_\lambda(\omega)\end{bmatrix}=\omega_\lambda(\omega)\begin{bmatrix} X_\lambda(\omega)\\ -Y_\lambda(\omega)\end{bmatrix}\ . \tag{3.9}$$

Since the operator in this equation is not Hermitian, Eq. (3.9) has to be supplemented by the adjoint eigenvalue problem, where $i\Gamma\rightarrow -i\Gamma$. The eigenvalues of the adjoint problem are $\omega_\lambda^*(\omega)$ with eigenvectors $[R_\lambda(\omega)S_\lambda(\omega)]$, say. One can then show that $-\omega_\lambda(-\omega)$ is also an eigenvalue of Eq. (3.9) with eigenvector $[S_\lambda^*(-\omega)R_\lambda^*(-\omega)]$. Likewise, $-\omega_\lambda^*(-\omega)$ is also an eigenvalue of the adjoint equation with eigenvector $[Y_\lambda^*(-\omega)X_\lambda^*(-\omega)]$.

One knows from general theory[8] that the poles of $F$ lie in the second and fourth quadrants of the complex energy plane. This means that the real and imaginary parts of the $\omega_\lambda(\omega)$ always differ in sign. Then the fact that $-\omega_\lambda(-\omega)$ is also an eigenvalue means that one can recover the complete spectrum of $F$ from a knowledge of the eigenvalues

$$\omega_\lambda(\omega)=\alpha_\lambda(\pm\omega)-i\beta_\lambda(\pm\omega)$$

in the fourth quadrant for both signs of $\omega$. This spectrum is indicated schematically in Fig. 3. The pattern of eigenvalues is not symmetric about the imaginary axis unless $\Gamma(\omega)=\Gamma(-\omega)$.

Since the eigenvalue problem (3.9) is not self-adjoint, the orthogonality relation is between the eigenvectors of the original and adjoint problem,

$$[R_\lambda^\dagger(\omega)S_\lambda^\dagger(\omega)]\begin{bmatrix} X_\lambda(\omega)\\ -Y_\lambda(\omega)\end{bmatrix}=\eta_\lambda\delta_{\lambda\lambda'}\ . \tag{3.10}$$

The phase $\eta_\lambda$ is $+1$ or $-1$ accordingly as the eigenvalue $\omega_\lambda(\omega)$ lies in the fourth or second quadrant. These results are proved by an extension of the method given by Thouless.[5]

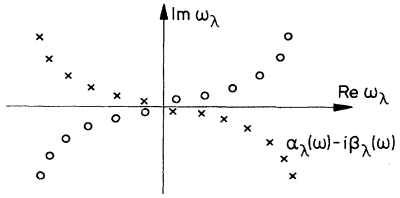


FIG. 3. Pattern of eigenvalues $\omega_\lambda(\omega)$ giving the poles of $F(\omega)$ (crosses). The eigenvalues $\omega_\lambda^*(\omega)$ of the adjoint problem are also shown (dots).

The solution of Eq. (3.8) can now be expressed as the sum

$$F=\sum_{\lambda}\frac{\eta_\lambda}{\omega-\omega_\lambda(\omega)}\begin{bmatrix}X_\lambda(\omega)\\ Y_\lambda(\omega)\end{bmatrix}[R^\dagger_\lambda(\omega)S^\dagger_\lambda(\omega)] \tag{3.11}$$

over all eigenstates. The individual submatrices of $F$ may then be read off, e.g.,

$$F_{ph,hp}=\sum_{\lambda}{}'\frac{X_\lambda(\omega)R^\dagger_\lambda(\omega)}{\alpha_\lambda(\omega)-i\beta_\lambda(\omega)-\omega}+\sum_{\lambda}{}'\frac{S^*_\lambda(-\omega)Y^{*\dagger}_\lambda(-\omega)}{\alpha_\lambda(-\omega)-i\beta_\lambda(-\omega)+\omega}\ , \tag{3.12}$$

where we have made use of the connection between the eigenvectors of $\omega_\lambda(\omega)$ and $-\omega_\lambda(-\omega)$ to write the sums over states with eigenvalues in the fourth quadrant only.

## IV. DOORWAY STATE CONTRIBUTIONS TO Σ

We now make the division of the self-energy into doorway and background contributions as suggested in Eq. (2.11), and calculate the doorway piece $\Sigma^d$ by inserting two versions of the polarization propagator F into Eq. (2.9). In the first calculation, we approximate $F$ by the noninteracting polarization propagator Π for independent particle-hole pairs.

### A. Noninteracting particle-hole pairs

We now calculate the contribution $\Sigma^d_1(\omega)$ to second order in the interaction using the dressed propagator $G^b_2$ and $\Pi(34,\omega)$. This corresponds to using doorway states consisting of noninteracting two-particle–one-hole excitations. The result, ignoring antisymmetry effects, is given by

$$\Sigma^d_1(\omega)=-i\sum_{234}|(32\,|\,V\,|\,41)|^2\int\frac{d\omega'}{2\pi}G^b_2(\omega-\omega')\Pi(34,\omega')\ . \tag{4.1}$$

While unrealistic in that interactions necessary for the buildup of collectivity in $\Sigma^d_1$ are absent, Eq. (4.1) gives results that are illustrative of the full problem. The energy integral can be evaluated using the Lehmann representation for $G^b_2$ again. The calculation is outlined in the Appendix and gives

$$\Sigma^d_1(\omega)=\sum_{234}|(32\,|\,V\,|\,41)|^2\left\{\frac{(1-n_2)(1-n_3)n_4}{\omega-\epsilon_2-\epsilon_3+\epsilon_4+i[W_2(\omega-\epsilon_3+\epsilon_4)+W_3(\omega-\epsilon_2+\epsilon_4)+W_4(\epsilon_3-\omega+\epsilon_2)]}+\frac{n_2n_3(1-n_4)}{\omega-\epsilon_2-\epsilon_3+\epsilon_4-i[W_2(\omega-\epsilon_3+\epsilon_4)+W_3(\epsilon_4+\omega-\epsilon_2)+W_4(\epsilon_3-\omega+\epsilon_2)]}\right\}. \tag{4.2}$$

It is evident from this expression that the damping of the doorway states is controlled by the *off-shell* values of $W_2$, $W_3$, and $W_4$. The arguments of these functions have been forced off-shell due to the sharing of the total energy $\omega$ between the various excitations in the intermediate state. [By off-shell, we mean, as usual, that the energy argument of a function like $W_1(\omega)$ does not equal the energy eigenvalue $\epsilon_1$ of the state 1.] For example, $W_2(\omega-\epsilon_3+\epsilon_4)$ in the first term of Eq. (4.2) describes the damping of a particle state 2 in the presence of a particle-hole excitation $(\epsilon_3-\epsilon_4)$, and therefore must be assigned the share $\omega-(\epsilon_3-\epsilon_4)$ of the available energy. One can verify the remaining energy arguments in Eq. (4.2) in the same way. This pattern of energy arguments in the $W$'s also ensures that the imaginary part of $\Sigma^d_1(\omega)$ changes sign properly as $\omega$ passes through the Fermi surface at $\lambda$. To be specific, consider the first term containing two-particle–one-hole excitations, where $2=m$ and $3=n$ are particle states, while $4=i$ is a hole state. The following pattern then appears in the imaginary part of the denominator.

$$W_m(\omega-\epsilon_n+\epsilon_i)+W_n(\omega-\epsilon_m+\epsilon_i)+W_i(\epsilon_m+\epsilon_n-\omega)\ . \tag{4.3}$$

According to Eq. (2.13), the first two terms are nonzero if $\omega-(\epsilon_n-\epsilon_i)$ and $\omega-(\epsilon_m-\epsilon_i)>\lambda$, while the third vanishes unless $\epsilon_m+\epsilon_n-\omega<\lambda$. Noting that combinations of the type $\epsilon_m-\lambda$ and $\epsilon_m-\epsilon_i$ are always positive, being single particle and particle-hole excitation energies, one sees that all three of these inequalities can only be met if $\omega$ is at least greater than $\lambda$. In a similar fashion, the imaginary part of the denominator in the second term of Eq. (4.2) only survives if $\omega<\lambda$, so that the sign of $\mathrm{Im}\Sigma^d_1(\omega)$ changes from negative to positive as $\omega$ passes through $\lambda$. Furthermore, each term in Eq. (4.3) switches on individually as its argument exceeds $\lambda$. This is shown schematically in Fig. 4.

Finally, each term in Eq. (4.3) goes on shell at the excitation energy $E_d=\epsilon_m+\epsilon_n-\epsilon_i$ of the two-particle–one-hole doorway state. The width of the doorway state

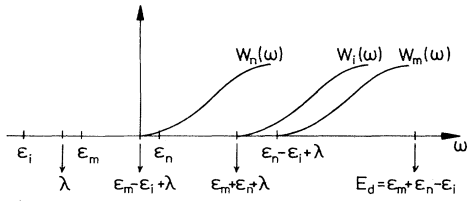


FIG. 4. Variation with energy of the absorptive components that enter into the damping calculation of a two-particle–one-hole state placed at $E_d=\epsilon_m+\epsilon_n-\epsilon_i$. The Fermi energy is at $\lambda$.

[given by twice the expression (4.3)] thus becomes a sensitive function of its excitation energy, a feature that will be essential in actual calculations. A similar pattern emerges for the damping of two-hole—one-particle excitations.

In the event that the doorway states in Eq. (4.2) were to become dense enough so that one could essentially average over them in some interval $\Delta$, one would retrieve Eq. (2.12) with

$$W_1=(\pi/\Delta)\sum_{\Delta}{}' |(32|V|41)|^2 ,$$

as expected.

### B. Particle-hole vibrations

We now include interactions among the particle-hole excitations, and replace Eq. (4.1) by

$$\Sigma_1^d(\omega)=-i\sum_{23456}|(62|V|51)|^2\int\frac{d\omega'}{2\pi}G_2^b(\omega-\omega')F(6543,\omega') . \tag{4.4}$$

Using the solutions (3.11) for $F$, one can again do the energy integral (see the Appendix). The final result, which involves the following abbreviations,

$$A_{12,\lambda}(\omega)=\left[\sum_{mi}x_{mi}^{\lambda}(\omega)(i1|V|m2)+\sum_{mi}y_{mi}^{\lambda}(\omega)(mi|V|i2)\right]\left[\sum_{nj}r_{nj}^{\lambda*}(\omega)(n2|V|j1)+\sum_{nj}s_{nj}^{\lambda*}(\omega)(j2|V|n1)\right] \tag{4.5}$$

and

$$B_{12,\lambda}(-\omega)=\left[\sum_{mi}x_{mi}^{\lambda}(-\omega)(i2|V|m1)+\sum_{mi}y_{mi}^{\lambda}(-\omega)(m2|V|i1)\right]\times\left[\sum_{nj}r_{nj}^{\lambda*}(-\omega)(n1|V|j2)+\sum_{nj}s_{nj}^{\lambda*}(-\omega)(j1|V|m2)\right] , \tag{4.6}$$

is given by

$$\Sigma_1^d(\omega)=\sum_{\lambda}{}'\sum_{2}\left[\frac{(1-n_2)A_{12,\lambda}(\omega-\epsilon_2)}{\omega-\epsilon_2-\alpha_\lambda+i\beta_\lambda+iW_2(\omega-\alpha_\lambda)}+\frac{n_2B_{12,\lambda}(\epsilon_2-\lambda)}{\omega-\epsilon_2+\alpha'_\lambda-i\beta'_\lambda-iW_2(\omega+\alpha'_\lambda)}\right] , \tag{4.7}$$

where the eigenvalues $\alpha_\lambda-i\beta_\lambda$ and $\alpha'_\lambda-i\beta'_\lambda$ are evaluated at arguments $\omega-\epsilon_2$ and $\epsilon_2-\omega$, respectively. The indexed lower case letters in Eqs. (4.5) and (4.6) denote components of the corresponding upper case column vector, e.g., $x_{mi}^{\lambda}(\omega)$ is the $(mi)$th component in $X_\lambda(\omega)$. At this stage, the sum on $\lambda$ involves the complete spectrum of $F$. However, in applications this will be restricted to a few low-lying collective modes, with the remaining $\lambda$'s being considered as absorbed into the background $\Sigma_1^b(\omega)$.

## V. INCLUSION OF ANGULAR MOMENTUM, ISOSPIN, AND PAIRING

In order to implement the general theory developed thus far, we must consider the various symmetry properties of actual nuclear states in addition to specifying a phenomenological form for $\Sigma_1^b(\omega)$ and a specific nuclear model in which to calculate $\Sigma_1^d(\omega)$.

### A. Angular momentum

In a spherical nucleus all single particle and hole states of the average nuclear field carry good angular momentum, as do the eigenvibrations that are built up from such interacting particle-hole pairs. Therefore, a state label like 1 specifies all the single particle quantum numbers $\{n_1l_1j_1m_1\}$ in the average field. In the following, we segregate the magnetic quantum number $m$, and write $\{1,m_1\}$, now reserving 1 as an abbreviation for the remaining nonmagnetic quantum numbers. Thus, for example, $F(4321,\omega)$ becomes

$$F(4m_43m_32m_21m_1,\omega)$$

in this notation.

Now consider the expression (2.9) that is represented by the second diagram in Fig. 2. Angular momentum conservation requires that the total angular momentum of the intermediate particle or hole plus vibration state couple to the angular momentum $j_1$ of state 1 under examination. It is therefore convenient to introduce an interacting particle-hole propagator $F^J$ carrying angular momentum $J$. This is given by

$$F^J(\vec{43}\vec{21},\omega)=\sum_{\substack{m_1m_2\\m_3m_4}}(j_4m_4j_3-m_3|JM)(-)^{j_3-m_3}F(4m_43m_32m_21m_1,\omega)(-)^{j_2-m_2}(j_1m_1j_2-m_2|JM) , \tag{5.1}$$

where the arrow notation on the left indicates the order in which the angular momenta are coupled in the Clebsch-Gordan coefficients. We use this notation generally. Then it is a matter of simple angular momentum algebra to show that $F^J(\vec{43},\overleftarrow{21},\omega)$ satisfies the following equation:

$$F^J(\vec{43}\overleftarrow{21},\omega)=\Pi(43,\omega)\left[\delta_{14}\delta_{23}-\sum_{56}(54\mid\tilde{V}\mid 63)F^J(\vec{65}\overleftarrow{21},\omega)\right], \tag{5.2}$$

a result that may be obtained formally from Eq. (3.7) by simply choosing the coupling scheme on the left, and then maintaining it throughout the equation. Note that $F^J$ is independent of $M$, and $\Pi(43,\omega)$ is independent of both $J$ and $M$, except that $j_4$ and $j_3$ must be able to couple to $J$. Then the self-energy of a state carrying angular momentum $j_1$ may be written in terms of $F^J$ as

$$\Sigma^d_{j_1}(\omega)=-i\sum_J\sum_{23456}\left[\frac{2J+1}{2j_1+1}\right](j_4j_1\mid V\mid j_3j_2)^*(j_5j_1\mid V\mid j_6j_2)\int\frac{d\omega'}{2\pi}G^b_2(\omega-\omega')F^J(\vec{65}\overleftarrow{43},\omega'), \tag{5.3}$$

where we have again neglected antisymmetry.

This result indicates that the contribution to $\Sigma^d_1$ from polarization propagators carrying a prescribed angular momentum are additive. One observes again that the result (5.3) follows formally from Eq. (2.9) by applying the "arrow coupling" technique, provided one includes a factor

$$(2J+1)/(2j_1+1)$$

that arises from recoupling. Therefore, the final result for $\Sigma^d_{j_1}(\omega)$ from Eq. (5.3) can be read off from Eq. (4.7) using the replacements $A_{12,\lambda}\rightarrow A^J_{12,\lambda}$ and $B_{12,\lambda}\rightarrow B^J_{12,\lambda}$ where $A^J_{12,\lambda}$ and $B^J_{12,\lambda}$ are given by Eqs. (4.5) and (4.6) with $(i\,1\mid V\mid m\,2)$ recoupled after including the factor

$$(2J+1)/(2j_1+1)$$

and summing on $J$. This result is recorded later in connection with Eq. (5.8).

### B. Isospin

The filled single particle levels of a nucleus with $N>Z$ may be divided into core levels occupied by both protons and neutrons, and valence levels that accomodate the excess neutrons. The ground state $\mid Z,N\rangle$ of this $A$ particle system carries isospin $[T_0,T_0]$ where $2T_0=N-Z$.

Adding a proton to, or removing a neutron from, the valence region likewise produces states of good isospin $[T_0-\frac{1}{2},\ T_0-\frac{1}{2}]$ in the residual $A\pm1$ systems. This is not the case, however, when a proton is added above or a neutron removed from below the valence shell. Then states of mixed isospin are formed. Let us examine the self-energy $\Sigma^d_1$ in this situation. If the index 2 on $G^b_2$ in the expression for $\Sigma^d_1$ is a neutron hole in the core, then not $G^b_2$, but rather the propagators $G^b_a$ and $G^b_{aa}$ for the analog and antianalog quasihole excitations are known, and have the simple form (2.14), e.g.,

$$G^b_{aa}(\omega)=[\omega-\epsilon_{aa}-\Sigma^b_{aa}(\omega)]^{-1}, \tag{5.4}$$

where $\epsilon_{aa}$ is defined such that $E_{aa}=\lambda-\epsilon_{aa}$ is the antianalog excitation energy. We introduce[15] the quasihole creation operators

$$\begin{aligned}\phi_a&=[-\mathrm{n}+\mathrm{p}T^{(-)}]/(2T_0+1)^{1/2},\\ \phi_{aa}&=\left[\mathrm{n}+\frac{\mathrm{p}T^{(-)}}{2T_0}\right][2T_0/(2T_0+1)]^{1/2}\end{aligned} \tag{5.5}$$

in terms of neutron (n) and proton (p) hole creation operators for the core region, and the isospin lowering operator

$$T^{(-)}=\sum_\nu p^\dagger_\nu n_\nu .$$

These operators create states of good isospin $[T_0\pm\frac{1}{2},\ T_0-\frac{1}{2}]$ corresponding to analog and antianalog states in $[Z,\ N-1]$ of the parent system $[Z-1,\ N]$. The relations (5.5) allow one to express $G^b_2$ as

$$G^b_2=\frac{2T_0}{2T_0+1}G_{aa}(\omega)+\frac{1}{2T_0+1}G_a(\omega) \tag{5.6}$$

when 2 refers to a neutron hole in the core. If we restrict the polarization bubble attached to $G^b_2$ to consist of isoscalar ($\Delta T=0$) excitations only, then isospin conservation requires that the state 2 has the same isospin as the state label 1 on $\Sigma^d_1$. Hence,

$$\Sigma^d_1=[2T_0/(2T_0+1)]\Sigma^d_{aa}$$

or

$$(2T_0+1)^{-1}\Sigma^d_a,$$

if 1 is an antianalog or analog quasihole, respectively. The self-energies $\Sigma^d_{aa}$ and $\Sigma^d_a$ are calculated from Eq. (2.9) as before with the replacements $G^b_2\rightarrow G^b_{aa}$ or $G^b_a$. We note in passing that the background contributions $\Sigma^b_{aa}$ and $\Sigma^b_a$ are quite different in these two Green's functions; $G^b_{aa}$ is subjected to essentially the full damping by the optical field,

$$\Sigma^b_{aa}=[2T_0/(2T_0+1)]iW_2,$$

while $\mathrm{Im}\Sigma^b_a\cong0$ because the level density of compound states with the same isospin as the analog state is expected to be much lower.[16]

### C. Pairing

So far we have assumed a sharp Fermi surface separating occupied and unoccupied single particle levels. This

distinction cannot be maintained in applications to the isotopes of tin, for example, which we discuss in the next section. It is well known that the valence shell neutrons in these isotopes exhibit strong pairing effects.[17] We take cognizance of this by introducing the standard Bogoliubov transformation[8] to quasiparticle creation and destruction operators, and expressing $G_2^b$ in terms of these. Then, for example, the propagator $G_2^{(0)}$ for a HF state 2 is replaced by

$$G_2^{(0)}(\omega)=\left[\frac{u_2^2}{\omega-E_2+i\eta}+\frac{v_2^2}{\omega+E_2-i\eta}\right], \tag{5.7}$$

where $E_2$ is the quasiparticle excitation energy

$$E_2=[(\epsilon_2-\lambda)^2+\Delta^2]^{1/2},$$

as measured from the quasiparticle vacuum, while $u_2$, $v_2$, and $\Delta$ are the probability amplitudes and gap parameter. The effect of pairing is thus to reduce the component of the Green's function associated with a HF particle or hole in state 2 from unity to $u_2^2$ or $v_2^2$, respectively. These two components are no longer mutually exclusive so that the line associated with $G_2^{(0)}$ in any diagram is partially a particle state and partially a hole state. This effect can be carried over into the dressed Green's function $G_2^b$ by substituting $u_1^2$ for $(1-n_1)$ and $v_2^2$ for $n_2$ in Eqs. (3.3) and (3.4) for the particle and hole strength functions of the background. This replacement leaves the sum rule (3.6) for the total strength unchanged, since $u_1^2+v_1^2=1$.

The calculation of the doorway self-energy that includes pairing and angular momentum effects follows the same pattern as that leading to Eq. (4.7). One finds

$$\Sigma_1^d(\omega)=\sum_\lambda{}' \sum_J \sum_2 \frac{(2J+1)}{(2j_1+1)}\left[\frac{A^J_{12,\lambda}(\omega-\lambda-\tilde{E}_2)u_2^2}{\omega-\lambda-\tilde{E}_2-\alpha_\lambda+i\beta_\lambda+iW_2(\omega-\alpha_\lambda)}+\frac{B^J_{12,\lambda}(\lambda-\tilde{E}_2-\omega)v_2^2}{\omega-\lambda+\tilde{E}_2+\alpha'_\lambda-i\beta'_\lambda-iW_2(\omega+\alpha'_\lambda)}\right], \tag{5.8}$$

where $\tilde{E}_2=(E_2-\Delta)$ is the pairing quasiparticle excitation energy relative to $\lambda$, and the arguments of $\alpha_\lambda$, $\beta_\lambda$ and $\alpha'_\lambda$, $\beta'_\lambda$ are now $\omega-\lambda-\tilde{E}_2$ and $\lambda-\tilde{E}_2-\omega$, respectively. This expression is simply obtained from Eq. (4.7) by the replacement of $\epsilon_2>\lambda$ in the first term in that equation by $\lambda+\tilde{E}_2>\lambda$, which is particlelike, and $\epsilon_2<\lambda$ in the second term by $\lambda-\tilde{E}_2<\lambda$, which is holelike. The factors $(1-n_2)$ and $n_2$ are replaced by the probabilities $u_2^2$ and $v_2^2$.

The expression (5.8) is generally applicable, since the pairing effects automatically disappear whenever the state 2 falls in the core region. Additional pairing effects can appear in the polarization propagator. This occurs when $F$ is made up of interacting quasiparticles, as has been discussed in some detail by Baranger.[18] We note in passing that since pairing leads to nonconservation of particle number, there must also be an associated fluctuation in isospin measured by $\langle T^2\rangle-\langle T\rangle^2$. If this quantity is small relative to $\langle T\rangle^2$, the consequences of isospin breaking are small. This inequality is well satisfied for the isotopes of Sn, which are considered next.

## VI. APPLICATION TO THE TIN ISOTOPES

In this section, we apply the formalism developed thus far to a calculation of the strength function for the isotopes of Sn. We must therefore specify (a) the HF single particle energies $\epsilon_1$ and the quasiparticle spectrum resulting from these for a given isotope, and (b) the self-energy insertions $\Sigma_1^b(\omega)$ and $\Sigma_1^d(\omega)$. We illustrate the implementation of these facets of the problem by describing the calculation of the $g_{9/2}$ strength function for the removal of a neutron from $^{116}$Sn.

### A. Single particle energies and the quasiparticle spectrum

The shell model single particle valence levels that are relevant[17] for discussing nuclear structure in the vicinity of the Sn isotopes are listed in Table I. The associated quasiparticle levels, shown on the right side of this table, were calculated using the common gap parameter $\Delta=0.92$ MeV, and the Fermi energy $\lambda=-9.67$ MeV. The neutron threshold (zero energy point) has been located by identifying the $3s_{1/2}$ quasiparticle state with the neutron separation energy in $^{116}$Sn. The filled $g_{9/2}$ to $f_{5/2}$ states do not enter the pairing calculation. We have taken the location of these from estimates of Gerlic.[7] The proton single particle levels have simply been obtained by shifting the last occupied proton level, the $g_{9/2}$ state to the Fermi energy $\lambda$, and are listed in Table II. The accuracy with which single particle energies are known does not warrant a better determination of the proton energies.

### B. The background self-energy

According to Eq. (2.12), we require the matrix elements

$$W_1(\omega)=\langle 1\,|\,W_{\rm opt}(\omega)\,|\,1\rangle .$$

To construct a plausible phenomenological form for these, we make appeal to Fermi liquid theory,[13] which predicts a $(\omega-\lambda)^2$ dependence of $W_1(\omega)$ near the Fermi surface, as well as the fact that the on-shell $W_1(\epsilon_1)$ is a slowly increasing function of $\epsilon_1$ near $\epsilon_1=0$. The simple form

$$W_1(\omega)=W_0\left[\frac{\omega-\lambda}{\lambda}\right]^2, \tag{6.1}$$

where $W_0$ is the value of the optical potential at $\omega=0$ (neutron threshold) agrees very well with the empirically determined on-shell variation of $W_1$ with energy.[19] Since this expression is meant to be an extrapolation to negative values of $\omega$ in the vicinity of the Fermi energy, Eq. (6.1) should not be confused with the empirically known energy dependence of the optical potential for positive energies. When 1 refers to a hole state, we continue to use the expression (6.1). This involves yet a further assumption,

TABLE I. The neutron spectrum. The single particle energies, measured from the zero (neutron threshold) and as excitation energies from $\lambda$ are given for the valence shell levels and first harmonic oscillator shell levels below this. The occupation probabilities $v_a^2$ and quasiparticle energies associated with the valence shell are also listed. These have simply been extended into the core region, by setting $v_a^2=1$ and $E_a=|\epsilon_a-\lambda|$. The $3s_{1/2}$ quasiparticle lies at excitation energy 0.11 MeV, where $s_n=9.56$ MeV is the neutron separation energy in $^{116}$Sn.

| Level | $\epsilon_a$ (MeV) | $\lvert(\epsilon_a-\lambda)\rvert$ (MeV) | $E_a$ (MeV) | $\tilde{E}_a=E_a-\Delta$ (MeV) | $v_a^2$ |
|---|---|---|---|---|---|
| $1h_{11/2}$ | −8.30 | 1.37 | 1.65 | 0.73 | 0.09 |
| $2d_{3/2}$ | −8.90 | 0.77 | 1.20 | 0.28 | 0.18 |
| $3s_{1/2}$ | −9.20 | 0.47 | 1.03 | 0.11 | 0.27 |
| $1g_{7/2}$ | −10.88 | 1.21 | 1.52 | 0.60 | 0.90 |
| $2d_{5/2}$ | −11.10 | 1.43 | 1.70 | 0.78 | 0.92 |
| $1g_{9/2}$ | −15.71 | 6.04 | | 6.04 | 1 |
| $2p_{1/2}$ | −16.01 | 6.34 | | 6.34 | 1 |
| $2p_{3/2}$ | −17.01 | 7.34 | | 7.34 | 1 |
| $1f_{5/2}$ | −18.01 | 8.34 | | 8.34 | 1 |
| $1f_{7/2}$ | −19.01 | 9.34 | | 9.34 | 1 |

also confirmed empirically,[19] that the spreading of single particle states on either side of the Fermi surface is similar. While as yet there is no specific proof of this assertion, it does seem a reasonable one in view of the fact that a particle or hole state at the same distance from the Fermi surface will be confronted with a similar density of compound levels.

Such a model for $W_1(\omega)$ is, of course, a gross approximation in a finite nucleus near $\omega=\lambda$, where, in contrast to a Fermi liquid, the very concept of an optical potential near the ground state looses all meaning, and we will have to see how these assumptions work in practice. In view of all these uncertainties, it is clearly futile to pay attention to the state dependence of $W$ as carried by the label 1. Thus we accept that Eq. (6.1) holds irrespective of whether the state label refers to a particle or a hole, so that $W_1(\omega)$ is symmetric about $\omega=\lambda$. The assumption of a specific form for $W_1(\omega)$ allows one to calculate this function at the various excitation energies required for the self-energy $\Sigma_1^d(\omega)$. We should perhaps emphasize that a more detailed analysis of the problem would introduce a phenomenological operator $W_{\text{opt}}$, calculate its matrix elements, and try to deduce its parameters from a match between theory and experiment, as has been done for $W_{\text{opt}}$ for positive energies.[2] At the present time, however, there is not enough systematic data to make such an analysis a definitive one.

TABLE II. The proton spectrum. This is obtained from the neutron single particle spectrum by moving the $g_{9/2}$ state to lie at $\lambda$.

| Level | $\epsilon_a$ (MeV) | $\lvert(\epsilon_a-\lambda)\rvert$ (MeV) |
|---|---|---|
| $1h_{11/2}$ | −2.26 | 7.41 |
| $2d_{3/2}$ | −2.86 | 6.81 |
| $3s_{1/2}$ | −3.16 | 6.51 |
| $1g_{7/2}$ | −4.84 | 4.83 |
| $2d_{5/2}$ | −5.06 | 4.61 |
| $1g_{9/2}$ | −9.67 | 0 |
| $2p_{1/2}$ | −9.97 | 0.30 |
| $2p_{3/2}$ | −10.97 | 1.30 |
| $1f_{5/2}$ | −11.97 | 2.30 |
| $1f_{7/2}$ | −12.97 | 3.30 |

### C. Structure of doorway states in $^{116}$Sn

Two types of doorway states present themselves as candidates in this nucleus. These consist of a single neutron hole coupled to vibrations of the proton core (type I), or neutron valence shell (type II), respectively. If, in the last case, these doorway states have their neutron hole in the core, then, as discussed in Sec. V B, such states do not by themselves conserve isospin. The correct linear combination for such type II doorway states is obtained[15] by forming the analog state of a proton hole coupled to neutron valence shell vibrations in the parent system $^{115}$In. It thus contains components more complex than two-particle—one-hole excitations. Hence the type I doorway state represents a dressing of the $g_{9/2}$ quasihole by *proton* vibrations, while the type II dresses the $g_{9/2}$ quasihole with neutron vibrations. In this picture, we have considered the proton core and neutron valence shell vibrations as occurring independently. This is not strictly true. The residual interaction will mix them. However, since the proton excitations are *inter*shell, while the neutron vibrations are *intra*shell, there is a relatively large energy separation ($\sim$2—4 MeV) between their respective excitation energies. Their mixing is consequently small. We continue to neglect it in what follows, and speak of these types of vibrations as though they occur as independent modes of excitation.

A common feature of the spectra of the tin isotopes is the occurrence of low-lying $2^+$ and $3^-$ collective modes. In $^{116}$Sn, these lie at $\hbar\omega_2=1.27$ MeV and $\hbar\omega_3=2.38$ MeV, respectively.[20] The expected positions of doorway states

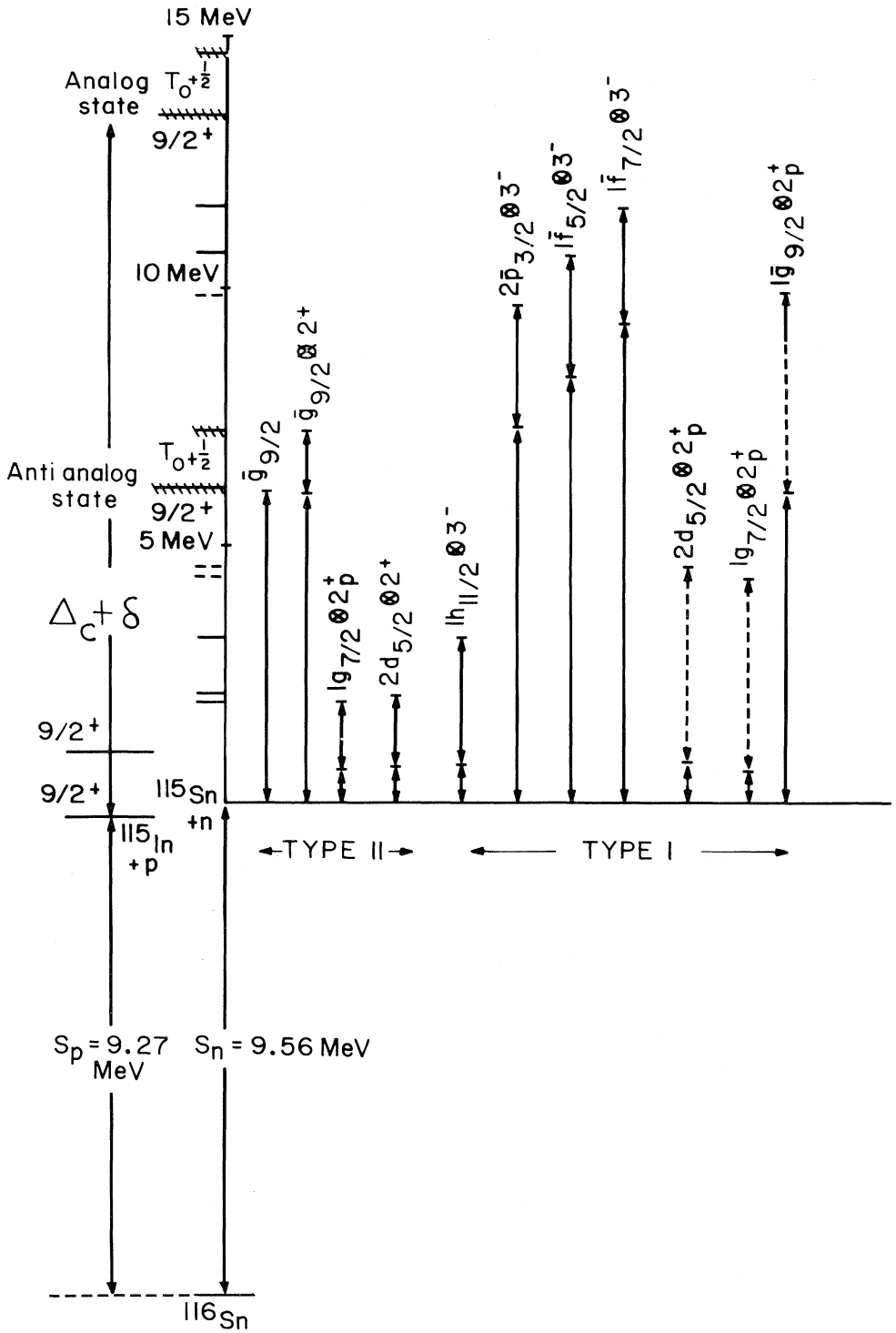


FIG. 5. Energy-level diagram showing the relation of the one hole plus vibration doorway states to the $g_{9/2}$ analog and antianalog states of $^{115}$Sn. The experimental neutron and proton threshold energies for $^{116}$Sn are also indicated. $\Delta_c$ and $\delta$ are the Coulomb energy shift and the neutron-proton energy difference, respectively. The horizontal lines on the vertical axis mark the projections of the individual one hole plus vibration levels that have been individually identified by the excitations that make them up. The barred letters indicate neutron quasiholes, unbarred letters neutron (pairing) quasiparticles. The $2^+$ and $3^-$ (experimental) collective modes at 1.27 and 2.38 MeV, respectively, are shown on top of the single quasihole or quasiparticle they are combined with to form a doorway. The dotted lines give the same information for the calculated $2^+_p$ (proton core) vibration. The $g_{9/2}$ analog and antianalog states and their accompanying doorways have been crosshatched for easy reference.

that can be formed by coupling these collective vibrations to those neutron hole states of Table I that can couple with them to a total angular momentum $\frac{9}{2}^+$ are shown in Fig. 5. The isobaric splitting[21] of the $g_{9/2}$ analog-antianalog pair is shown for comparative purposes. The estimated positions of type I doorways, based on a calculated value of $\hbar\omega_2 \simeq 3.8$ MeV (see later) for a $2^+$ collective mode of the proton core is shown by the broken lines. We have arbitrarily grouped those doorways involving the known $3^-$ excitations under type II, i.e., mainly proton vibrations. Whether this is predominantly so or not, is not relevant for our further discussion, since these doorway states lie too far from the $g_{9/2}$ quasihole to be significant.

It is clear from the level diagram in Fig. 5 that the $g_{9/2}$ quasihole state remains isolated except for the $[\bar{g}_{9/2}\otimes 2^+]$ doorway just above it. The reasons for this are simply either the strong compression of the neutron quasiparticle spectrum or the large binding energies of the neutron quasiholes in the core. Both effects favor either low-lying or high-lying doorway states. The latter lie at too low an excitation energy for the damping mechanism in our model to be physically realistic, while the former are effectively spread out to merge with the background because the model *is* certainly realistic in this region. To illustrate this effect, let us estimate the damping width of the component

$$2\bar{p}_{3/2}\otimes[2d_{5/2}2\bar{p}_{1/2}]$$

of the doorway state at 10 MeV excitation that contains the $3^-$ vibration. One has, from the second term in Eq. (4.2), that the on-shell half-width of such a two-hole—one-particle state is given by

$$W_{2\bar{p}_{3/2}}(\epsilon_{2\bar{p}_{3/2}})+W_{2d_{5/2}}(\epsilon_{2d_{5/2}})+W_{2\bar{p}_{1/2}}(\epsilon_{2\bar{p}_{1/2}})=1 \text{ MeV} ,$$

which is of the same order as the half-width of the $g_{9/2}$ quasihole (0.86 MeV).

Experimentally,[7] the $g_{9/2}$ quasihole strength function (see Figs. 7 and 8) shows significant fragmentation on its low energy side. We show that this data is consistent with the presence of doorway states of the type II, consisting of a $2^+$ collective mode due to vibrations of the proton core coupled to neutron holes. We estimate the position and strength of this collective mode from an RPA description of the proton core excitations, using the previously determined $P_2$ part of the residual interaction that describes the neutron valence shell vibrations so successfully.[17] This interaction may be written as

$$V(12)=-f_J Y_J(1)\cdot Y_J(2) ,$$

where $Y_{JM}$ is a spherical harmonic of rank $J$ and $f_J$ and adjustable (but for our case known) interaction strength. Its direct matrix elements cause the transfer of angular momentum $J$ during particle-hole collisions. They are

$$(32\,|\,V\,|\,41)=-f_J Q^J_{\bar{4}3} Q^J_{2\bar{1}} ,$$

where $Q^J_{2\bar{1}}$ is the multipole moment of order $J$.

It is well known[5] that the eigenvalue equation Eq. (3.10) for the RPA collective modes can be solved exactly if we approximate the direct matrix elements in that equation by the separable form just given, and drop the exchange matrix elements. Then the RPA collective mode excitation energy becomes

$$\omega_c(\omega)=\mathscr{E}(\omega)\left[1-\frac{2f_J}{\mathscr{E}(\omega)}\sum_{mi}(Q^J_{mi})^2\right]^{1/2} . \tag{6.2}$$

The symbol

$$\mathscr{E}(\omega)=E-i\Gamma(\omega)$$

gives the average energy of the dressed particle-hole excitations that make up the vibrations $\omega_c$. In particular, a $2^+$ mode (which we henceforth designate $2^+_p$) can be built up out of the proton excitations $1g_{9/2}\rightarrow 2d_{5/2}$ and $1g_{9/2}\rightarrow 1g_{7/2}$. The high degeneracy of the $g_{9/2}$ state (containing $2j+1=10$ protons) ensures the collective nature of the resulting vibration. To calculate its energy, we note by reference to Table II that the unperturbed energies of the above excitations are nearly degenerate: they lie at 4.6 and 4.8 MeV, respectively, while their individual (on-shell) half-widths are

$$W_m(\epsilon_m)+W_i(\epsilon_i)=2.2(4.6/9.67)^2=0.50 \text{ MeV}$$

and

$$2.2(4.8/9.67)^2=0.54 \text{ MeV} ,$$

respectively, using $W_0=2.2$ MeV. This gives an average on-shell half-width of $\Gamma=0.52$ MeV. Hence,

$$\mathscr{E}=(4.7-0.52i) \text{ MeV} .$$

Actually, the imaginary part of $\mathscr{E}$ is energy dependent. Using Eq. (6.1) for $W_1(\omega)$ to construct an average $\Gamma(\omega)$ and setting $f_J=2.50$ MeV, a value bracketed by Kisslinger and Sorensen's value[17] of 2.75 MeV, and the Bohr-Mottelson estimate[22] of 2.04 MeV for the quadrupole-quadrupole strength, one finds the values of

$$\omega_c(\omega)=\alpha_c(\omega)-i\beta_c(\omega)$$

given in Fig. 6. Note that the real part of the collective energy is lowered from 4.7 MeV to around 3.8 MeV by an amount almost independent of $\omega$, while the imaginary part, $\beta_c(\omega)$, depends strongly on $\omega$.

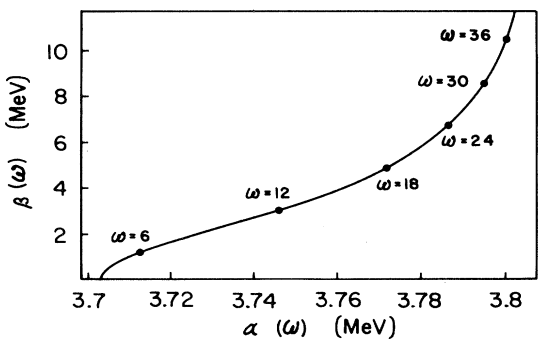


FIG. 6. Plot of $\beta_c$ vs $\alpha_c$ as a function of the energy parameter $\omega$. Values of $\omega$ at 2 MeV intervals are indicated.

It now remains to couple the $2_p^+$ state to intermediate neutron hole (and/or quasiparticle) states. Using $\mathrm{Re}\omega_c \cong 3.8$ MeV, we obtain the set of dashed energy levels shown in Fig. 5.

It is important to note that we use the same interaction, viz., $-f_J Y(1)\cdot Y(2)$ for coupling the RPA dressed bubble $F^J(\vec{43}\overleftarrow{21},\omega)$ to the intermediate neutron state as was used to generate the bubble. The collective enhancement of the coupling matrix elements $A^J_{12,\lambda}$ and $B^J_{12,\lambda}$ is seen directly from the result that $A^J_{12,\lambda}$ and $B^J_{12,\lambda} \sim \sum_{mi} (Q^J_{mi})^2$ for separable interactions.

Having calculated $\Sigma_1^d(\omega)$ in this fashion, we add it to $\Sigma_1^b(\omega)$ in accordance with Eq. (2.11) and hence construct $G_1(\omega)$ of Eq. (2.2). The strength function is then given by

$$S_1(\omega) = \frac{1}{\pi}\mathrm{Im}G_1(\omega) \ . \tag{6.3}$$

This result refers to the isospin channel $T_0 - \frac{1}{2}$. The neutron component of this,

$$S_1(\omega)\times 2T_0/(2T_0+1) \ ,$$

is to be compared with the experimental data.

## VII. RESULTS

In this section we show results of calculating the $g_{9/2}$ neutron hole strength from Eq. (5.8) and make a comparison with experiment. Figures 7 and 8 show this strength function for the isotope $^{115}$Sn, for two choices of the strength $W_0$. The parameters entering the calculation have been described in Sec. VI. In these, and in all subsequent figures, the experimental data of Gerlic *et al.*[7] have been shown as (i) a dashed histogram of the original data averaged over 0.5 MeV bins, and (ii) when there is sufficient data, as a dotted curve representing the measured strength smoothed with a running Breit-Wigner weight function of half-width 0.3 MeV. The main peak observed in these two figures shows the $1g_{9/2}$ antianalog state,

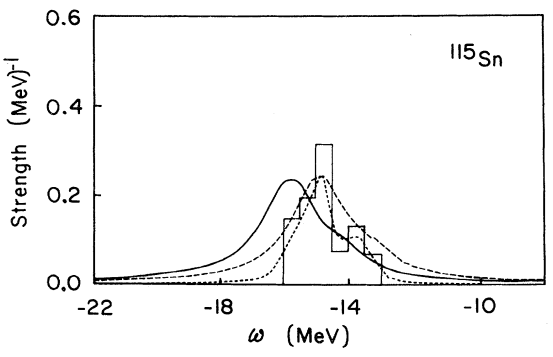


FIG. 7. Calculated strength function for the $1g_{9/2}$ antianalog neutron hole state in $^{115}$Sn. The solid curve shows the calculation for $W_0=2.8$ MeV and $f_J=2.50$ MeV, that determines the width and splitting of the giant resonance. The dashed curve shows the same calculation, but with all neutron single particle energies moved up by 0.9 MeV. The experimental data of Gerlic *et al.*[7] is indicated both as a histogram and as a dotted curve, see text.

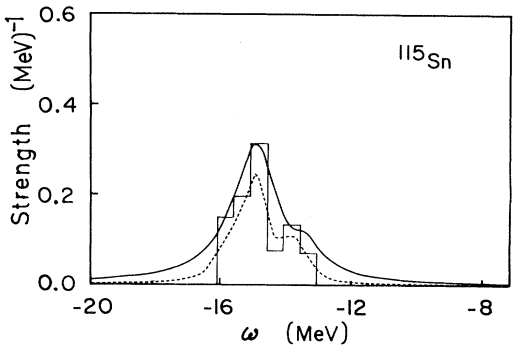


FIG. 8. The $g_{9/2}$ strength function as calculated in Fig. 7, but with $W_0=2.2$ MeV. The neutron single particle levels have been shifted up by 0.9 MeV.

while the shoulder immediately to the right of this is due to the two overlapping doorway configurations $2d_{5/2}\otimes 2_p^+$ and $1g_{7/2}\otimes 2_p^+$ (see Fig. 5) that have been shifted slightly due to their mutual interaction. The main peak of the calculated strength is not properly positioned using the single particle energies listed in Tables I and II; see Fig. 7. Since these energy values are parameters in the shell model, one can readjust the calculated peak to lie at the observed position. We have done this by simply raising all neutron single particle energies by a common amount, 0.9 MeV.

It is clear from these two figures, that an excellent description of the observed strength function is obtained from the model we have proposed. Not only is the splitting of the $g_{9/2}$ hole correctly reproduced by the coupling strength $f_J$ that is determined independently from other data, but also the widths of both the main peak and its doorway satellite are correctly described. It is a matter of opinion which of the two calculations, which differ only in the value of the parameter $W_0$, give a better representation of the data.

It is also of interest to see what the model predicts for the $g_{9/2}$ strength function for the other isotopes of Sn. Referring back to Eq. (5.8) for the doorway self-energy $\Sigma_1^d(\omega)$, one sees that the only quantities entering this equation that are strongly dependent on mass number are the quasiparticle excitation energies $E_a$, the occupation probabilities $u_a^2$ and $v_a^2$, and $\lambda$. Published calculations[17] of these allow one to follow the variation of these parameters through the Sn isotopes. Two examples of such strength functions are shown in Fig. 9 for $^{111}$Sn and $^{119}$Sn.

Two features should be pointed out: (i) The doorway state shifts in energy as one moves through the Sn isotopes. This is brought about by the mass number dependence of the quasiparticle energies $E_a$. (ii) The fits predicted for $^{111,119}$Sn are satisfactory, without further adjustment of the remaining parameters that were used for $^{115}$Sn.

We conclude this section by pointing out that the other doorway states appearing in Fig. 5 have little effect on the $g_{9/2}$ quasihole due to their energy separation or (on the high energy side) large damping. It is of interest to note, however, that two of the three low-lying doorways formed by coupling the $2^+$ or $3^-$ vibration to the $2d_{5/2}$, $1g_{7/2}$,

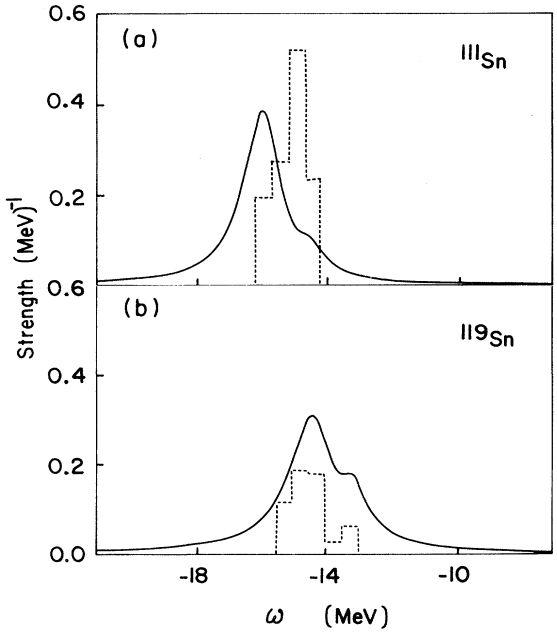


FIG. 9. (a) Calculated $1g_{9/2}$ strength function for $^{111}$Sn, using parameters $\lambda=-11.44$ MeV and $\Delta=0.97$ MeV. (b) Calculated $1g_{9/2}$ strength function for $^{119}$Sn, using parameters $\lambda=-9.12$ MeV and $\Delta=1.05$ MeV. The other parameters have remained the same as those used in Fig. 8 for both these calculations.

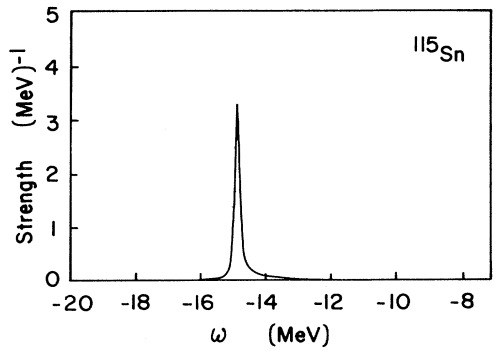


FIG. 10. Calculated $1g_{9/2}$ strength function for $^{115}$Sn, using parameters as in Fig. 8. The background self-energy $\Sigma_1^b(\omega)$ has been suppressed in $G_1(\omega)$.

and $1h_{11/2}$ neutron quasiparticle have been identified with observed states $\frac{9}{2}^+$ at 2.37 and 3.07 MeV in the pickup data of Gerlic *et al.*[7]

## VIII. DISCUSSION AND OUTLOOK

While the results of the model for calculating the strength function for deep-lying holes and their comparison with experiment are self-evident, some concluding remarks are in order. We first examine the basic assumption that the self-energy can be split into a smoothly-varying piece $\Sigma_1^b(\omega)$ and a doorway piece $\Sigma_1^d(\omega)$. The two extremes of this assumption are the following. (i) There is no background contribution. All damping of the hole state proceeds via doorway states to which it is coupled locally. One can easily test this idea by shutting off $\Sigma_1^b(\omega)$ in $G_1(\omega)$ but not in $G_1^b(\omega)$. This is shown in Fig. 10. The resulting peak height of the $g_{9/2}$ state is seen to be much too high, and the width much too narrow. (ii) There is no doorway contribution. $\Sigma_1^d(\omega)$ is zero. Then the $g_{9/2}$ strength function obviously consists of a single unsplit peak.[15]

The question of how $\Sigma_1^b(\omega)$ behaves with energy is a second basic assumption. The device of relating $\mathrm{Im}\Sigma_1^b(\omega)$ to $W_1(\omega)$, the average value of the nuclear optical potential at energy $\omega$ is certainly a reasonable one, especially in view of the excellent results that have been obtained from it. From a more fundamental point of view, the implementation of this assumption is more troublesome: experiment does not give us information on the "off-shell" values of $W_1(\omega)$ when $\omega\neq\epsilon_1$. We have circumvented this problem by arguing that details of how $W_1(\omega)$ depends on its state label "1" could not be implemented in our calculations in view of the sparseness of data. While this is certainly true, the question is a very interesting one that will certainly have to be answered as more data becomes available that *does* require a better knowledge of $W_1(\omega)$. The situation has a strong parallel with the development of the optical potential at positive energies. After the initial phenomenological success, the availability of more and better data has resulted in rather detailed empirical knowledge of the properties of the nuclear absorptive potential. This empirical detail has also provided the necessary impetus to carry out a reasonably successful derivation of the nuclear optical potential from a microscopic point of view.[23] In the case of hole states one can expect developments as more data become available. For deep-lying holes, development of a microscopic theory would be of special interest, since the off-shell behavior of $W_1(\omega)$ enters into the determination of the doorway state spreading widths in an essential way.

## ACKNOWLEDGMENTS

We would like to thank Dieter Heiss for many stimulating discussions. One of us (S.P.K.) thanks African Explosives Chemical Industries, Proprietary, and the Council for Scientific and Industrial Research for financial assistance.

## APPENDIX

We sketch the arguments underlying the approximate evaluation of $\Sigma_1^d(\omega)$ from Eq. (4.1). Since we eventually invoke the approximate expressions (3.3) and (3.4) for the strength functions, it is clear that the intermediate state 2 in the frequency integral

$$\int \frac{d\omega'}{2\pi} G_2^b(\omega-\omega')F(6543,\omega') \tag{A1}$$

is either a particle or a hole. Let us assume it is a particle and insert the approximation $\Pi$ for $F$ as in Eq. (4.1). Then,

$$\int \frac{d\omega'}{2\pi} G_2^b(\omega-\omega')\Pi(34,\omega') = \sum_s |(c_2^\dagger)_{s0}|^2 \frac{(1-n_3)n_4}{\omega-\lambda-\epsilon_s-\epsilon_3+\epsilon_4+i[W_4(\epsilon_3-\omega+\lambda+\epsilon_s)+W_3(\epsilon_3+\omega-\lambda-\epsilon_s)]} . \quad \text{(A2)}$$

The symbols in this expression have already been defined in the main text. If we replace the $s$ sum by an integral, then the result (3.3) for $|(c_2^\dagger)_{s0}|^2$ may be used. This resonates at $\epsilon_s=\epsilon_2-\lambda$. Its cofactor in Eq. (A2) resonates at $\epsilon_s=\omega-\lambda-\epsilon_3+\epsilon_4$. We argue as in Eq. (3.2) and evaluate the $W$'s in each factor at the resonance of the other one. Hence $W_2(\epsilon_s+\lambda)\to W_2(\omega-\epsilon_3+\epsilon_4)$ in $|(c_2^\dagger)_{s0}|^2$, while $W_3(\epsilon_3-\omega+\lambda-\epsilon_s)\to W_3(\epsilon_4+\omega-\epsilon_2)$ and $W_4(\epsilon_3-\omega+\lambda+\epsilon_s)\to W_4(\epsilon_3-\omega+\epsilon_2)$. The remaining integration over $\epsilon_s$ is now elementary. A similar procedure holds if 2 is a hole state, and one obtains the result (4.2) quoted in the text.

The evaluation of (A1) when $F$ includes the interactions between particle-hole pairs follows a similar pattern. Instead of (A2), one is confronted with the expression

$$\sum_s (c_2^+)_{s0}|^2 \frac{A_{12,\lambda}(\omega-\lambda-\epsilon_s)}{\omega-\lambda-\epsilon_s-\alpha_\lambda(\omega-\lambda-\epsilon_s)+i\beta_\lambda(\omega-\lambda-\epsilon_s)} \quad \text{(A3)}$$

if 2 is a particle state. We use the same argument as in the derivation of (A2), i.e., evaluate $\alpha_\lambda$ and $\beta_\lambda$ at the resonance energy $\epsilon_s=\epsilon_2-\lambda$ of $|(c_2^\dagger)_{s0}|^2$ and $W_2$ in this factor at the resulting resonance energy $\epsilon_s=\omega-\lambda-\alpha_\lambda(\omega-\epsilon_2)$ of its cofactor in (A3). The remaining $\epsilon_s$ integral is again elementary and one obtains for (A3) the value

$$\frac{A_{12,\lambda}(\omega-\epsilon_2)(1-n_2)}{\omega-\epsilon_2-\alpha_\lambda(\omega-\epsilon_2)+i\beta_\lambda(\omega-\epsilon_2)+iW_2[\omega-\alpha_\lambda(\omega-\epsilon_2)]} \quad \text{(A4)}$$

which, together with a similar expression that holds if 2 is a hole state, leads to Eq. (4.7).


[1] H. Feshbach, C. E. Porter, and V. F. Weisskopf, Phys. Rev. 96, 448 (1954).

[2] I. Uhlehla, G. Ladislav, and Z. Pluhar, *Optical Model of the Atomic Nucleus* (Academic, New York and London, 1964).

[3] H. Feshbach, A. K. Kerman, and R. H. Lemmer, Ann. Phys. (N.Y.) 41, 230 (1967); B. Block and H. Feshbach, *ibid.* 23, 47 (1963).

[4] F. J. W. Hahne and W. D. Heiss, Ann. Phys. (N.Y.) 89, 68 (1975).

[5] D. J. Thouless, Nucl. Phys. 22, 78 (1961).

[6] C. B. Dover, R. H. Lemmer, and F. J. W. Hahne, Ann. Phys. (N.Y.) 70, 458 (1972).

[7] E. Gerlic, G. Berrier-Ronsin, G. Duhamel, S. Gales, E. Hourani, H. Langevin-Joliot, M. Vergnes, and J. van de Wiele, Phys. Rev. C 21, 124 (1980).

[8] See, for example, A. L. Fetter and J. D. Walecka, *Quantum Theory in Many-Particle Systems* (McGraw-Hill, New York, 1971).

[9] A. B. Migdal, *Theory of Finite Fermi Systems and Applications to Atomic Nuclei* (Interscience, New York, 1967).

[10] C. A. Engelbrecht, F. J. W. Hahne, and W. D. Heiss, Ann. Phys. (N.Y.) 104, 221 (1977).

[11] See, for example, R. D. Mattuck, *A Guide to Feynman Diagrams in the Many-Body Problem* (McGraw-Hill, New York, 1976).

[12] H. Feshbach, Ann. Phys. (N.Y.) 5, 357 (1958); 19, 278 (1962).

[13] D. Pines and P. Nozières, *The Theory of Quantum Liquids* (Benjamin, New York, 1966), p. 63.

[14] V. G. Soloviev, C. H. Stoyanov, and A. I. Vdovin, Nucl. Phys. A342, 261 (1980); P. F. Bortignon and R. A. Broglia, *ibid.* A371, 405 (1981); G. F. Bertsch, P. F. Bortignon, R. A. Broglia, and C. H. Dasso, Phys. Lett. 80B, 161 (1979), and further references cited therein.

[15] S. P. Klevansky and R. H. Lemmer, Phys. Rev. C 25, 3137 (1982).

[16] E. H. Auerbach, C. B. Dover, A. K. Kerman, R. H. Lemmer, and E. H. Schwartz, Phys. Rev. Lett. 17, 1184 (1966).

[17] L. S. Kisslinger and R. A. Sorensen, K. Dan. Vidensk. Selsk. Mat.-Fys. Medd. 32, No. 9 (1960); D. R. Bès, in *Proceedings of the International School of Physics, "Enrico Fermi" Course LXIX, Elementary Modes of Excitation in Nuclei,* edited by A. Bohr and R. A. Broglia (North-Holland, Amsterdam, 1977), p. 55.

[18] M. Baranger, Phys. Rev. 120, 957 (1960).

[19] C. Mahaux and H. Ngô, Phys. Lett. 100B, 285 (1981).

[20] *Advances in Nuclear Physics,* edited by M. Baranger and A. Vogt (Plenum, New York, 1969), Vol. 2, p. 129.

[21] A. M. Lane and J. M. Soper, Nucl. Phys. 37, 663 (1962).

[22] A. Bohr and B. R. Mottelson, *Nuclear Structure* (Benjamin, Reading, Mass., 1975), Vol. II, p. 418.

[23] *Microscopic Optical Potentials,* Lecture Notes in Physics 89, edited by H. V. von Geramb (Springer, Heidelberg, 1979).